NRL REPORT 3599

PHYSICAL OPTICS OF METAL PLATE MEDIA
PART 2, EXPERIMENTAL STUDIES

B. A. Lengyel and A. J. Simmons
Naval Research Laboratory

J. J. Brady, M. D. Pearson and S. Peoples
Oregon State College

January 3, 1950

Approved by:

Dr. L. C. Van Atta, Head, Antenna Research Branch
Dr. John M. Miller, Superintendent, Radio Division I

NAVAL RESEARCH LABORATORY
CAPTAIN F. R. FURTH, USN, DIRECTOR
WASHINGTON, D.C.

CONTENTS

ABSTRACT

An experimental study has been made of the transmitting and reflecting properties of metal-plate media with the plane of incidence perpendicular to the edges of the plates. The magnitude of the reflection coefficient was measured at normal incidence on the modified Michelson interferometer, and the phase change in transmission, on a free-space dielectrometer. At oblique incidence, transmitted and reflected intensities were measured on a microwave analogue of the spectrometer. The results provide an experimental confirmation of the theory of Carlson and Heins treated in NRL Report 3534.

PROBLEM STATUS

This final report completes the work on the problem.

AUTHORIZATION

NRL Problem R09-40R
NR 509-400

FOREWORD

A study of the reflecting and transmitting properties of metal-plate media was undertaken by the Antenna Research Branch of the Naval Research Laboratory as part of a program directed toward the investigation of microwave lenses and lens materials.

In an earlier report (NRL Report 3534) the theory of Carlson and Heins was extended. Numerical values of the reflection and transmission coefficients obtained from this theory were tabulated as functions of the parameters of the medium and the angle of incidence. In the present report experimental results are compared with theoretical predictions.

The results at oblique angles were obtained by Professor Brady and Messrs. Pearson and Peoples working at Oregon State College under NRL contract N173s-11303. The results at normal incidence were obtained by Dr. Lengyel and Mr. Simmons at the Naval Research Laboratory. The two sets of experimental information were correlated with the theory of Carlson and Heins by Dr. Lengyel.

L. C. Van Atta

PHYSICAL OPTICS OF METAL PLATE MEDIA
PART 2, EXPERIMENTAL STUDIES

INTRODUCTION

The theoretical foundation for wave propagation in the presence of parallel-plate metal structures was laid in the report entitled "Physical Optics of Metal Plate Media, Part 1,"[1] hereafter cited as Part 1. The object of the present work is to test experimentally the predictions of the theory regarding the reflection and transmission coefficients of metal-plate media. Both in Part 1 and in all experiments reported here, it has been deemed expedient to restrict the scope of the investigation by requiring that the surface of the medium be perpendicular to the metal plates and that the E-vector be parallel to their edges.

The theory is based on the assumptions that the plates are infinitely conducting and that their thickness is zero. The first of these assumptions poses no practical difficulty but the second cannot be approximated closely in an actual experiment.

The reflection and transmission measurements at normal incidence require a technique totally different from that practical at oblique incidence. The subdivision of this report is determined in part by this difference in technique and in part by the fact that the two types of experiments were performed in widely separated laboratories. All experimental work has been carried out in the 3 cm band largely because this is the frequency region for which apparatus of convenient size can be built.

EXPERIMENTS AT NORMAL INCIDENCE

Description of Equipment

The reflection and transmission measurements were performed on slabs of metal-plate media such as shown in Figure 1. The large dimensions facing the transmitter were in all cases about 30 x 30 cm (12″ x 12″). The plate separation, a, the depth of the slab, d, and the thickness of the plates, t, varied from slab to slab as shown in Table 1. The last column of this table shows the plate spacing $a' = a + t$.

The plates were made of brass and mounted on a heavier frame. In spite of all precautions it was not possible to keep them perfectly straight and for this reason the plate separation varied from point to point, the deviations reaching ±0.015 cm from the design value. Slab 4 was more accurate mechanically than slabs 1, 2, and 3.

---

[1] Lengyel, B. A. "Physical Optics of Metal Plate Media, Part 1 - Theoretical Considerations," NRL Report 3534, Sept. 19, 1949.

TABLE 1
Dimensions of the Metal-Plate Slabs in Centimeters

Slab No.	d	a	t	a′
1	3.20	1.847	.080	1.927
2	4.80	1.847	.080	1.927
3	9.60	1.847	.080	1.927
4	4.00	2.000	.075	2.075

A specially built frequency-stabilized, square-wave-modulated signal generator was the source of radiation. It operated between 2.9 and 3.6 cm, providing a $2a/\lambda$ ratio from 1.03 to 1.28 for slabs 1, 2, and 3 and a ratio from 1.11 to 1.38 for slab 4. A bolometer or crystal served as a detector in conjunction with a Radiation Laboratory Mark IV amplifier and a Ballantine voltmeter.

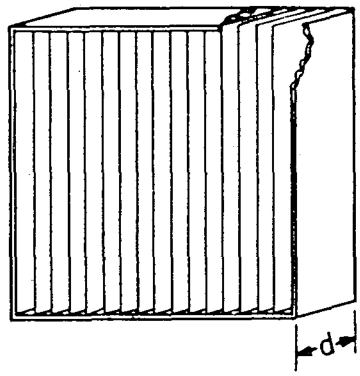

Figure 1 - Metal plate slab

The reflection measurements were made on a modified Michelson interferometer.[2,3] This instrument is shown in Figure 2 with its transmitting horn at the left. The beam was split by the half-reflecting glass sheet in center and only the radiation passing through the mirror was used. The signal reached the receiving horn in the rear after being reflected by the metal-plate slab and again by the half-reflecting glass sheet. It was then united with a reference signal from the transmitter led through a waveguide and a variable attenuator. With the aid of this attenuator the reference signal was adjusted to be equal in amplitude to the signal arriving through the open branch of the interferometer with a brass plate in place of the slab to be measured.

When the brass plate was removed and the metal-plate slab substituted, the reflection coefficient of the slab was determined by moving the slab in the direction of its normal and observing the ratio of the maxima to the minima in the detector. The calculation of the magnitude of the reflection coefficient was then performed as if the measurements had been made on an ordinary standing-wave detector.

In order to minimize unwanted diffraction and interference some thought was given to the choice of apertures and distances. The horns were at a distance of 120 to 140 cm from the reflecting surfaces, therefore within the Fresnel region of the slab regarded as a single aperture, D^2/λ being around 280 cm. On the other hand, they were in the far field of the individual channels, a^2/λ being less than 1.3 cm; therefore the departure of the radiation from a plane wave was no longer significant. Viewed from the horn, the reflecting

---

[2] *Lengyel, B. A., "A Michelson-Type Interferometer for Microwave Measurements," Proc. IRE 37, 1242-1244, 1949*

[3] *Lengyel, B. A. and Simmons, A. J., "An Interferometer for Microwaves," NRL Report No. 3562, 1949*

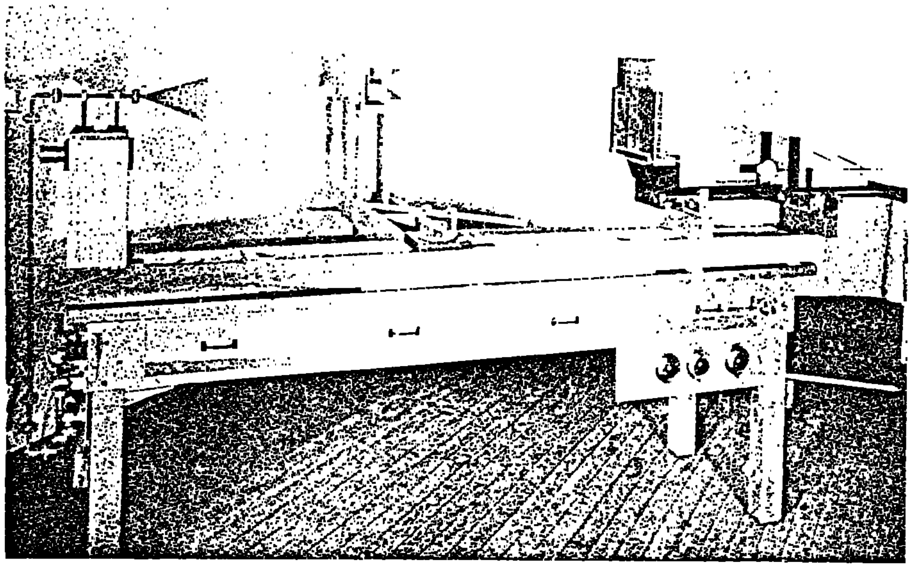

Figure 2 - Measurement of reflection at normal incidence

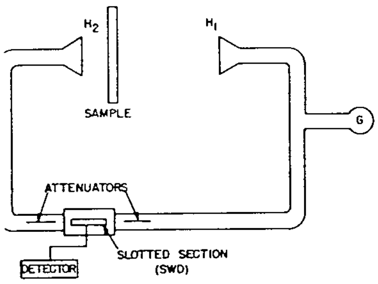

igure 3 - Diagram of apparatus for measurement of phase change in transmission

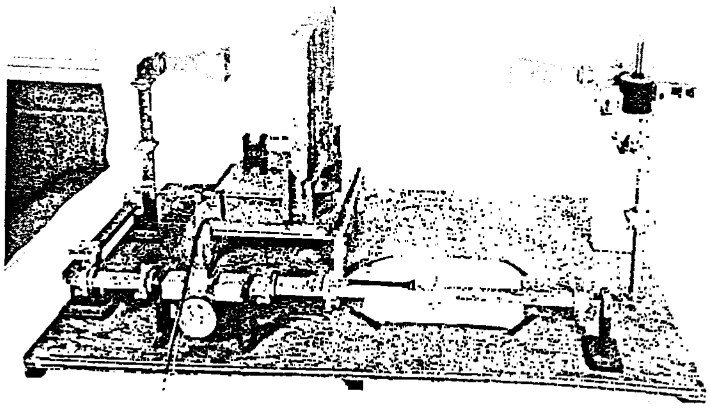

Figure 4 - Measurement of phase change in transmission

ırface was well within the first Fresnel zone, a position which seems important because ıe horn-reflector distance is varied during measurement.

The phase change in transmission through a metal-plate slab was measured on a free-ɔace dielectrometer which is a modification of an instrument of Redheffer[4] designed for ıe measurement of dielectric constants in free space. A schematic diagram and a photo-raph are shown in Figures 3 and 4 respectively.

A signal is radiated from horn H_1, received by horn H_2 and transmitted through a wave-uide containing attenuators and a standing-wave detector. A reference signal propagating

Montgomery, C. G., "Technique of Microwave Measurements," Rad. Lab. Ser. Vol. 11, p. 591, w York, 1947 in the opposite direction in the guide combines with the first signal to produce a standing-wave pattern. The attenuators are adjustable so that a high standing-wave ratio may be produced in the slotted section. When a dielectric or a metal-plate slab is interposed between the horns, the phase of the first signal is altered and the minima in the standing-wave detector are shifted. The performance of this instrument is limited by multiple reflections between the test slab and the horns. When the measurements are made at normal incidence, as in this case, the reflections become a serious source of error especially when the index of refraction is significantly different from one. The error of the measurement is a periodic function of the position of the slab with respect to the receiver, the period being one half of a wavelength. It can therefore be minimized by taking two measurements with the slab displaced by a quarter-wavelength and averaging the results.

Measurement of the Reflection Coefficient

The primary quantities derived from the theory are the transmission and reflection coefficients of the air-metal-plate interface. These quantities are not directly measurable on the slabs available for the experiment since reflections from the back surface of the slabs combine with those from the front surface. The resulting multiple reflections lead to a transmission and a reflection coefficient for the entire slab which depend on the depth (thickness) of the slab. Mathematical expressions for these coefficients were derived in Part 1. For the magnitude of the reflection coefficient the following expression was found: (Equation 66)

$$|R| = \frac{2\rho|\sin\psi|}{\sqrt{(1-\rho^2)^2 + 4\rho^2\sin^2\psi}},$$

where ρ is the magnitude of the reflection coefficient on the air-metal-plate interface, $\psi = \rho'' + \delta_2$, ρ'' is a phase function tabulated in Part 1 (p. 30) and $\delta_2 = 2\pi nd/\lambda$ is the phase delay between the front and back surfaces of the slab. All quantities entering into the expression for $|R|$ are functions of d or of $2a/\lambda$. The letter n stands for the index of refraction of the medium. Values of $|R|$ calculated for the four experimental slabs of Table 1 are presented as the solid curves in Figure 5.

To emphasize the role of the phase change occurring at the air-metal-plate medium interface, $|R|$ was also calculated assuming, in analogy to true dielectric materials, that no such phase change takes place. This hypothesis is equivalent to setting $\rho'' = \pi$. It results in the dotted curves of Figures 5(a) and (b).

Experimental values for $|R|$ were obtained for the four slabs. The slab depth, d, was fixed for each slab, the quantity $x = 2a/\lambda$ was varied by changing λ, and $|R|$ was measured as a function of x. The results, plotted as the points in Figure 5, are found to be in obvious disagreement with the dotted curves, but in reasonable agreement with the solid curves calculated from the Carlson-Heins theory. In appraising the agreement of experimental values of $|R|$ with those deduced from the theory, one must keep in mind the deviations of the metal-plate structure from the mathematical idealization and the errors inherent in the technique of measurement.

The finite conductivity of the plates is a source of loss within the slab. Therefore waves reflected from the back surface can never completely cancel waves reflected from the front surface. When this is taken into account, the solid curves in Figure 5 are modified so that they will no longer touch the axis $|R| = 0$. This effect, however, is practically negligible since the loss in the metal plate medium is only about 0.06 db/meter.

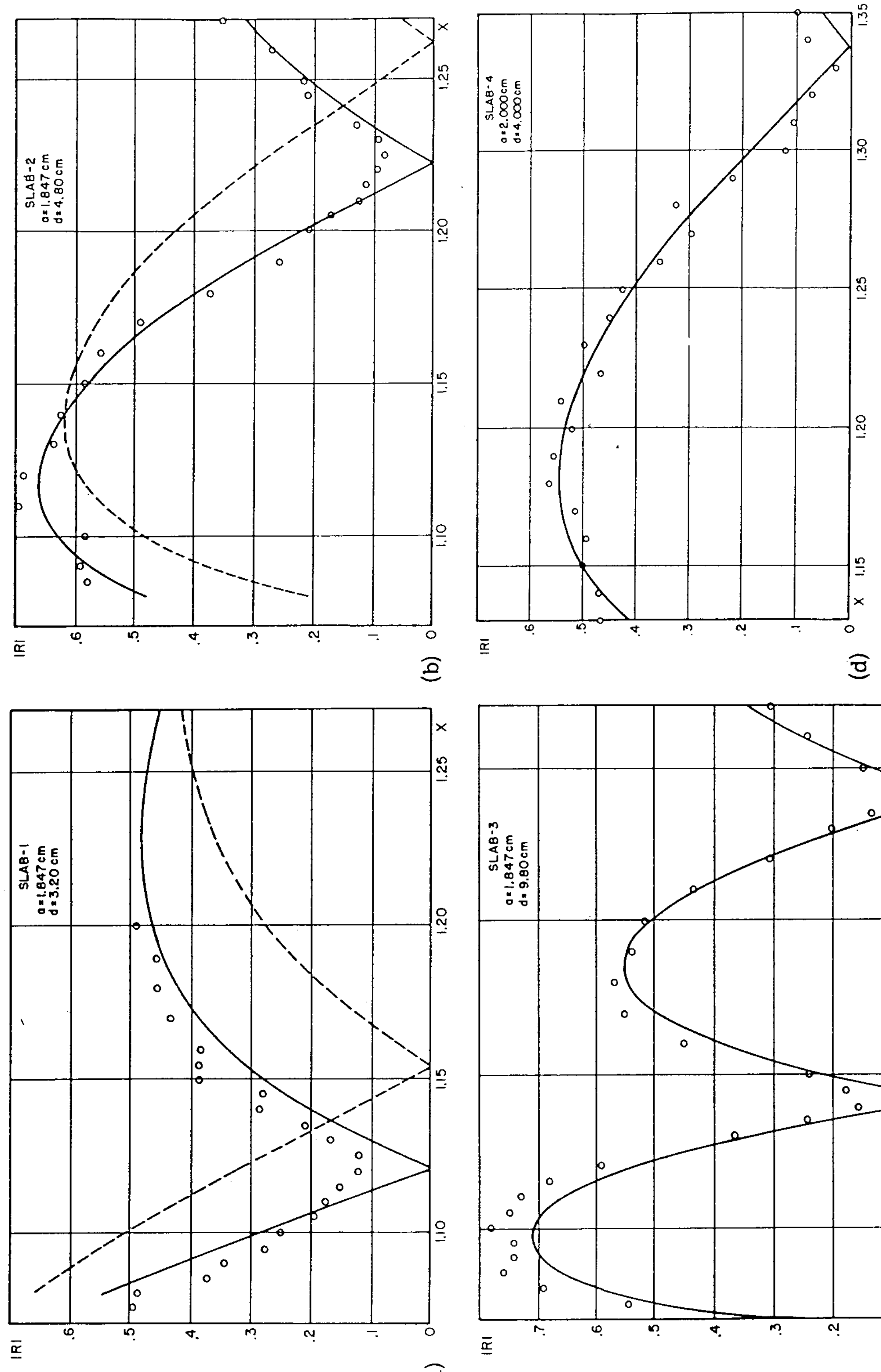

(Solid line: |R| calculated from the Carlson-Heins theory.
Dotted line: |R| calculated neglecting phase change on interface.)

Figure 5 - Reflection from slabs at normal incidence as a function of $x = 2a/\lambda$

The finite thickness of the plates gives rise to another systematic error which has not been evaluated theoretically. It seems, however, that with the dimensions chosen as they were at normal incidence this effect is very small.

A random error results from the variation of the spacing from one channel to the other due to the bending or buckling of the plates. Such variation is especially objectionable when the wavelength approaches the "cutoff" wavelength, 2a, because when x is close to one, $n = \sqrt{1 - x^{-2}}$ varies rapidly with a. To minimize such difficulties the measurements were restricted to the region $n > 0.37$, corresponding to the region $x > 1.08$. Spacers were introduced to give the structure rigidity and to hold the proper spacing within narrow tolerances. It was found that these spacers have to be very thin, 2 mm or less, otherwise they cause an appreciable reflection. The variation of the plate spacing was below 0.005λ, resulting in a variation in n of less than 0.013 in the middle of the band and less than 0.02 for the longest wavelength. Fortunately the errors introduced by a slight random buckling of the plates are partially self-compensating since the total width of the structure is determined by a rigid frame.

The principal systematic errors inherent in the measurement technique are those caused by diffraction, by the divergent character of the radiation, and by the presence of unwanted reflections. By careful choice of the dimensions of the apparatus, the effect of diffraction was reduced to negligible proportions. The divergence of the radiation introduced a spread in the angle of incidence amounting to $\pm 6°$ in the extreme. The effect due to this spread is very small since the reflection is not sensitive to angle near normal incidence. Furthermore, the effect is somewhat reduced since the amplitude of the signal decreases from its maximum value at the center to about 65% of this value at the edge.

The largest error is due to reflection from the carriage of the interferometer. This reflection introduces an error both in the normalization and in the actual measurement. It can be shown that the error in $|R|$ due to a carriage reflection of magnitude α is approximately

$$\alpha \left| -1 + e^{i\phi} R \right|$$

where ϕ depends on the position of the slab with respect to that of the normalizing solid plate.[5] Since the phase of R varies slowly with λ, this error depends on the wavelength. One may expect that in certain wavelength regions the measured value of $|R|$ will lie consistently above, in other regions below, its correct value. This error could be greatly reduced by taking two measurements at each wavelength with the slab moved by $\lambda/4$ with respect to the carriage. This was not done since the expected increase in precision did not warrant the additional effort required. The carriage reflection of the interferometer used remained below 0.05 over the entire 3-cm band; therefore the average error of the measurement of $|R|$ was less than 0.05, and the maximum error less than 0.10.

Small reflections from fixed objects did not seriously interfere with the measurement since they were simply added to the reference signal which was adjusted with each change of wavelength. Naturally, every reasonable effort was made to keep reflections in the room low, since radiation reflected successively from outside objects and the moving parts of the interferometer produces an uncompensated error.

Random errors did not seem large enough to mask the conspicuous agreement with the theoretical values. For a detailed analysis of these errors it is necessary to refer to the report on the interferometer.[6]

---

[5] *Lengyel and Simmons, op. cit., p. 13*

[6] *Lengyel and Simmons, op. cit.*

Measurement of Phase Change in Transmission

The quantity measured was the change of phase of a signal propagating between two horns (Figure 4) when a slab of metal-plate medium was interposed. The theoretical expression for this quantity was derived in Part 1 (Equations 71 and 72):

$$T' = \rho' + \psi' + \pi - \delta_1,$$

where ρ' is a function of $x = 2a/\lambda$, tabulated in Part 1, $\delta_1 = 2\pi d/\lambda$, and

$$\tan \psi' = \frac{1 + \rho^2}{1 - \rho^2} \tan \psi.$$

Values of ρ, the magnitude of the reflection coefficient of an air metal-plate medium interface, are tabulated in Part 1. Actually T', ρ', and ρ'' are determined up to a multiple of 2π only. If the tabulated values of ρ' and ρ'' are used, and if it is desired to obtain the least value of T' for a slab of negligible depth, then the following equation should be used:

$$T' = \rho' + \psi' - \pi - \delta_1.$$

Values of T', calculated for the four experimental slabs of Table 1, are presented as the solid curves of Figure 6 for comparison with the experimental points. The dotted curves represent the values of T' calculated assuming $\rho'' = \pi$. Again the experiments demonstrate that this assumption is not tenable.

The principal sources of error are mechanical imperfections of the slabs and unwanted reflections. The horns were only about 60 cm apart; therefore diffraction effects were negligible. The divergence of the beam, on the other hand, was greater than in the case of the reflection measurements. Multiple reflections between horns and the slab, and internal reflections within the closed system (consisting of waveguide sections, attenuators, and horns) were the most disturbing factors. Each measurement was repeated with the slab moved by a quarter wavelength and the average phase change was plotted.

Some information about the internal consistency of the experimental data may be gained by an examination of Figure 6d. The experimental points marked by circles were obtained first, then the spacers on the slab were exchanged for new and thinner ones, an attenuator in the dielectrometer was exchanged for one better matched, and the measurements were repeated. The experimental points finally obtained are marked by crosses. The mean deviation from the theoretical values is 0.10 radian or about 3% of the measured phase change.

EXPERIMENTS AT OBLIQUE INCIDENCE

Description of Equipment

Two metal-plate slabs of different construction were employed for measurements at oblique incidence. The first (#5) was similar to the slabs described in Part 1, except for the lack of the heavy frame. The plates were held together by long bolts, accurately machined spacers maintaining the required plate separation. The second slab (#6) was an assembly of equal lengths (9″) of square waveguide held together by a wooden frame. This slab was built in order to permit the measurement of reflection on a single surface. Wooden absorbing wedges were placed in each guide section to eliminate back surface reflection.

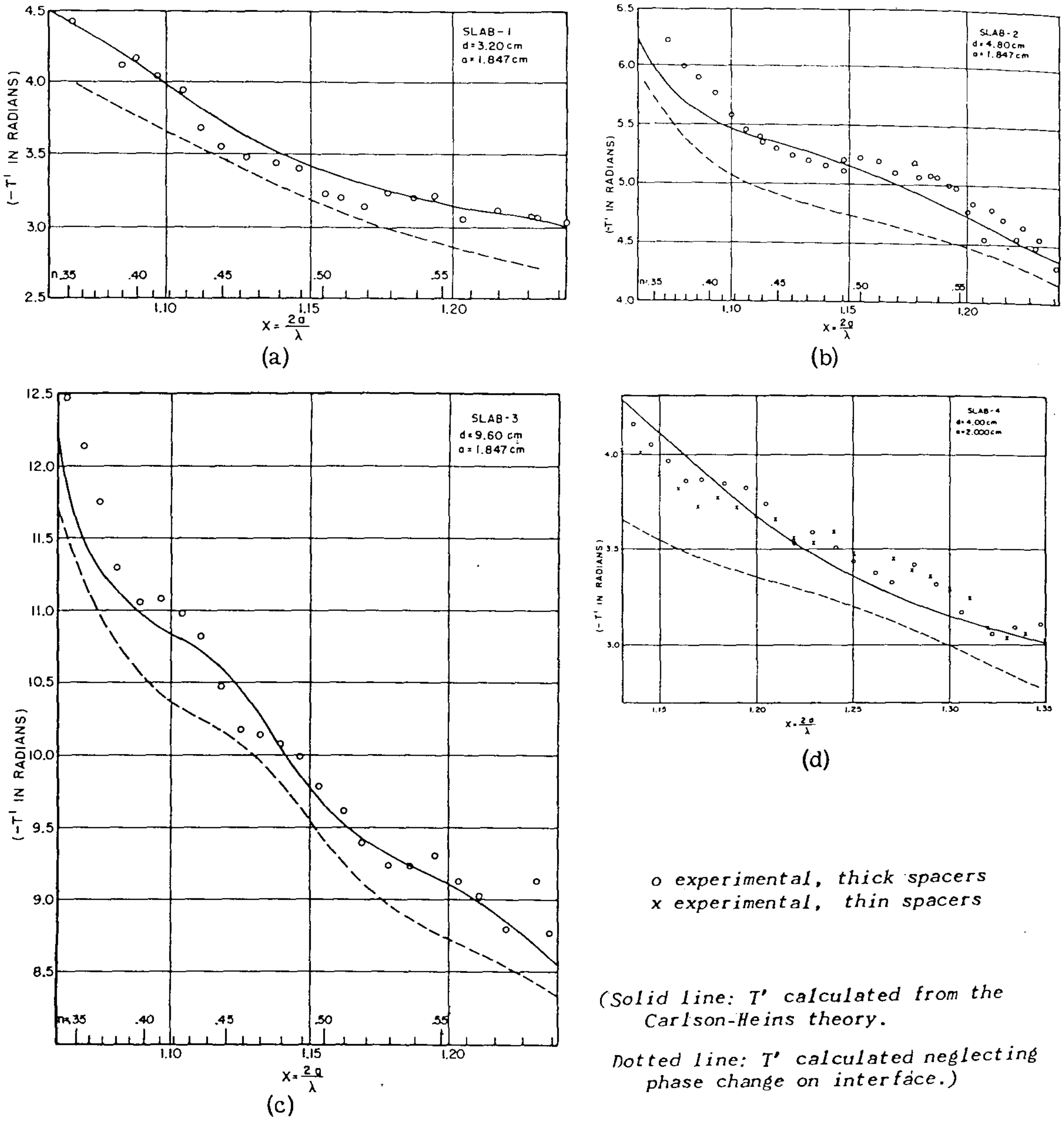

Figure 6 - Phase change in transmission at normal incidence

Figure 7 is a photograph of this assembly; Figure 8 shows an individual guide section and an absorbing wedge. Table 2 contains the relevant dimensions of these slabs.

An MIT Radiation Laboratory signal generator (419) employing three klystron tubes provided the radiation. This generator permitted the covering of the 3.1 to 3.7 cm wavelength band. The detection of the signal was accomplished as at normal incidence, except for the fact that provision was made for recording the data on a tape by means of an automatic recorder. The system was so designed that the vertical deflection of the trace on the tape was proportional to the power received.

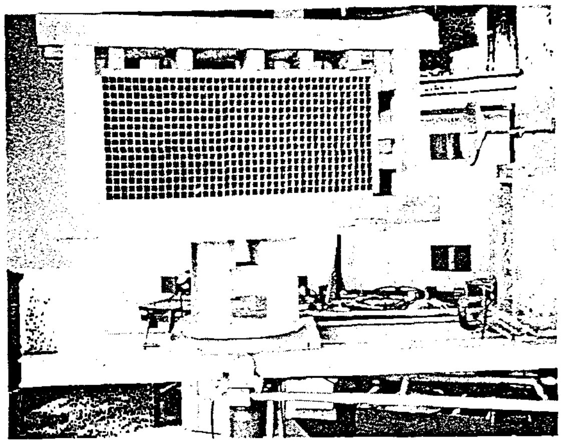

Figure 7 - Waveguide assembly (slab 6)

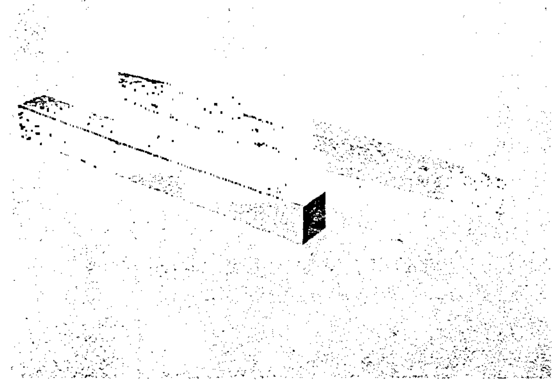

Figure 8 - Guide section and matching wedge

TABLE 2
Dimensions of the Metal-plate Slabs in Centimeters

Slab No.	Face*	d	a	t	a′
5	84.5 x 35.7	22.86	2.159	0.063	2.222
6	84.5 x 35.7	22.225	2.141	0.081	2.222

* *The measurements were made with the short sides of the face parallel to the E-vector.*

A spectrometer-like apparatus was constructed with a fixed transmitting paraboloid antenna (8″ diam.) and a rotating arm carrying the receiving horn. This apparatus is shown in Figures 9 and 10 which contain all relevant dimensions.

The movable arm was rotated slowly by a motor through a gear reduction drive and the received power was recorded on a tape moving in synchronism with the receiving horn. Precautions were taken to insure accurate identification of the angular position of the horn from the markings on the recording tape. The horn could swing over an arc of 340° leaving 10° clearance on each side of the transmitting antenna.

In every experiment the slab was set for a fixed angle of incidence and the receiver arm was rotated to obtain a pattern of the reflected and transmitted radiation. When a reflection pattern was taken, the slab was so positioned that the axis of rotation was in its front surface. For transmission measurements the slab was positioned with the axis in its back surface. In order to obtain both transmission and reflection measurements on the same tape, the instrument was stopped at the proper point and the slab was moved forward or back, keeping its orientation unchanged. This displacement of the slab was always accompanied by a corresponding displacement of the transmitter necessary to preserve their distance.

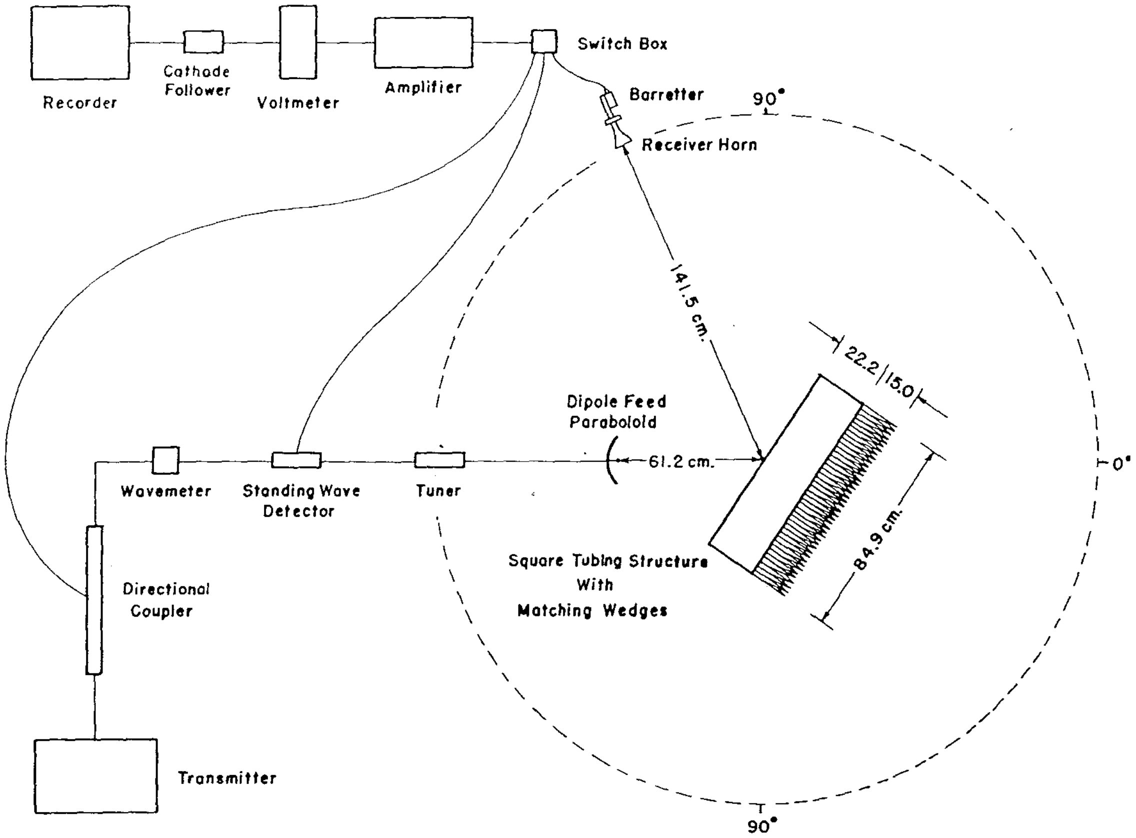

Figure 9 - Diagram of apparatus for oblique incidence

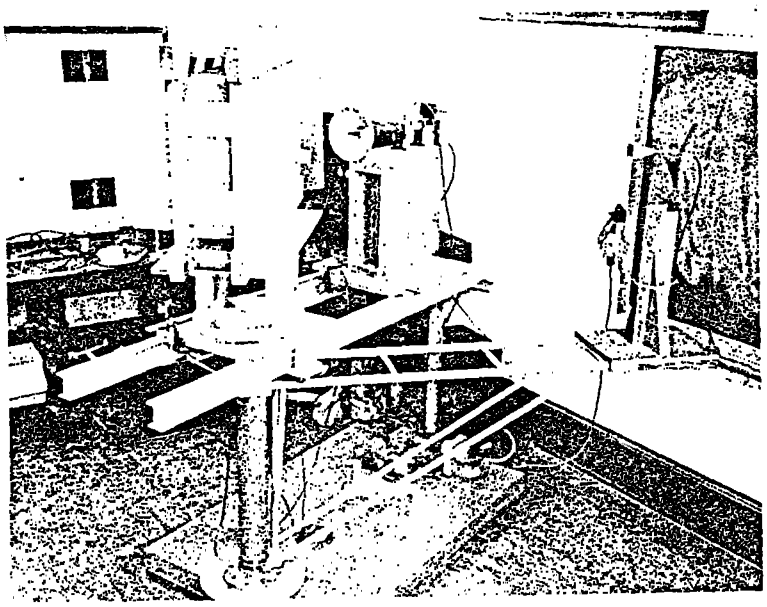

Figure 10 - Spectrometer with slab 6

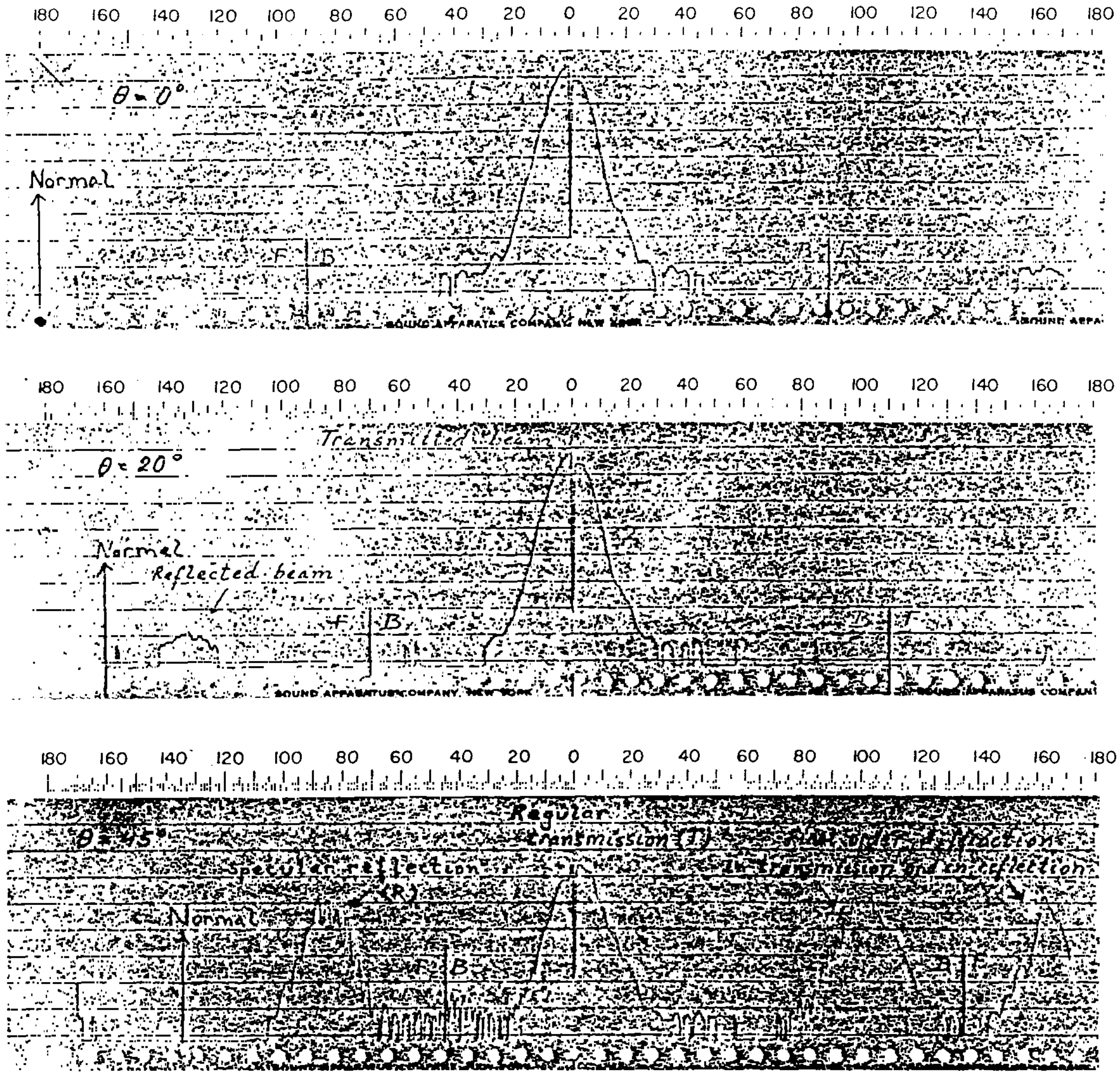

Figure 11 - Samples of records obtained with slab 5

Figure 11 shows samples of the record tape obtained with Slab 5. The transmitting antenna was always at 180° on the scale shown. The letters F and B refer to the front and back surfaces respectively, indicating which one contained the axis of rotation. The position of the angular zero is marked by the sharp dip of the trace, caused by the action of a microswitch, which connected the recorder to a fixed reference voltage of 0.3 volt at the instant the spectrometer arm passed the null position.

Measurements

It is in the nature of these experiments that rather wide lobes are obtained on the record tape, extending 10 to 15 degrees on each side of their maxima. These maxima are poorly defined because of the fine structure of the lobes. For this reason the experimental definition of reflection and transmission coefficients was not based on the comparison of maxima, but on the areas under the curves. Since all measurements were in terms of power, and since the metal-plate medium is essentially lossless, it seemed practical to speak of power reflection and transmission coefficients rather than of amplitude coefficients. The (power) reflection coefficient was defined experimentally as the ratio of the area under a reflected lobe to the area under the main lobe received with the slab removed from the path of the radiation. This definition required a separate determination of the latter area for each wavelength used. In addition, all data were normalized to a constant monitor reading. As a check on the normalization process a solid metal plate was placed in front of the slab and its reflected pattern was obtained. When the area under the reflected lobe of this pattern was used as the denominator of the expression for the reflection coefficient, the values agreed within a few percent with those obtained by the previous method.

When the angle of incidence θ is less than the limiting angle θ_L defined by the equation:

$$1 + \sin \theta_L = \lambda/a'$$

the theory predicts the presence of a single reflected beam at an angle equal to the angle of incidence. More precisely, the incident- and the reflected-wave normals are oriented at θ and $\pi - \theta$ respectively. This is the case of specular reflection, so well known in geometrical optics. When $\theta \geq \theta_L$, then in addition to the wave propagating in the direction $\pi - \theta$, diffracted waves will be present. In the cases of practical interest there is only one diffracted beam; the direction θ' of its wave normal is specified by the equation:

$$\sin \theta + \sin \theta' = \lambda/a' \quad .$$

The theory is based on the assumption that the plates have zero thickness, therefore plate separation a and plate spacing a′ are identical. In experimental work these quantities are slightly different. While propagation between the plates depends on a, diffraction grating effects depend on a′.

It has been shown theoretically that the intensity of specular reflection decreases gradually as θ varies from 0 to θ_L, and then rises very sharply.[7] The angle of incidence for which the reflection coefficient is a minimum should then coincide with the angle for which the diffracted beam first appears.

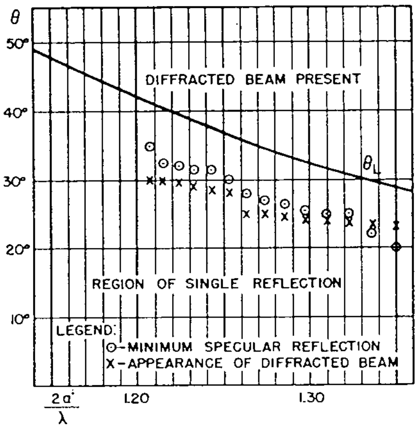

Figure 12 - The least angle of incidence permitting a diffracted beam

The observed angular position of the specular reflection coincides with the position predicted by the theory. The diffracted beam, however, makes its first appearance for an angle of incidence smaller than θ_L. This fact is brought out in Figure 12 where the minima of the intensity of specular reflection are also shown. The apparent discrepancy is understandable in view of the fact that the experiment is not performed with parallel beams; therefore the angle of incidence varies over the surface of the slab. The diffracted beam will appear when conditions for its appearance are satisfied on any one part of the reflecting surface. Moreover, when the diffracted beam first appears it has a broader power pattern than the incident beam, because of the small apparent size of the reflector when viewed from

[7] *Cf. Part 1, pp. 14 and 22.*

the direction of the diffracted beam. This fact further enhances the early appearance of the diffracted signal in the receiver. Finally, from the asymmetrical nature of the curves representing the reflection coefficient as a function of the angle of incidence,[8] it follows that the minimum of the reflected intensity will be shifted toward smaller mean angles of incidence when a divergent incident beam is used in place of a parallel beam.

Because of the interaction of the front and back surface reflections, the measurements on Slab 5 do not lend themselves directly to the calculation of the reflection coefficient of a single surface. It is, however, possible to calculate the reflection coefficient of the slab from the basic data furnished by the theory and this could then be correlated with the measured values. This was not done; a correlation was made between the theory and the data obtained on Slab 6 instead. The substitution of a square guide assembly for the ordinary metal-plate medium was justified experimentally since without absorbent wedges Slab 6 behaved like Slab 5. The effectiveness of the absorbers is clearly indicated by the contrast of the reflection coefficient vs. frequency curves with and without absorbers shown in Figure 13. The curve obtained without absorbers is essentially identical with that obtained on Slab 5. For $\theta = 15^0$ the theoretical curve has been calculated and was found to be in fair agreement with the curves shown in Figure 13.

Representative values of the single-surface power reflection-coefficient measured on Slab 6 are shown in Figure 14, and details are presented in Table 3. For angles of incidence of 10 to 25 degrees, the measured value of the reflection coefficient is consistently below the value predicted by the theory (solid curves). This apparent discrepancy is, no doubt, due to the fact that a parallel beam was not used in the experiment. It is likely that the measurements are subject to a systematic error which is more apparent in the case when $|r|$ is small than when $|r|$ is large.

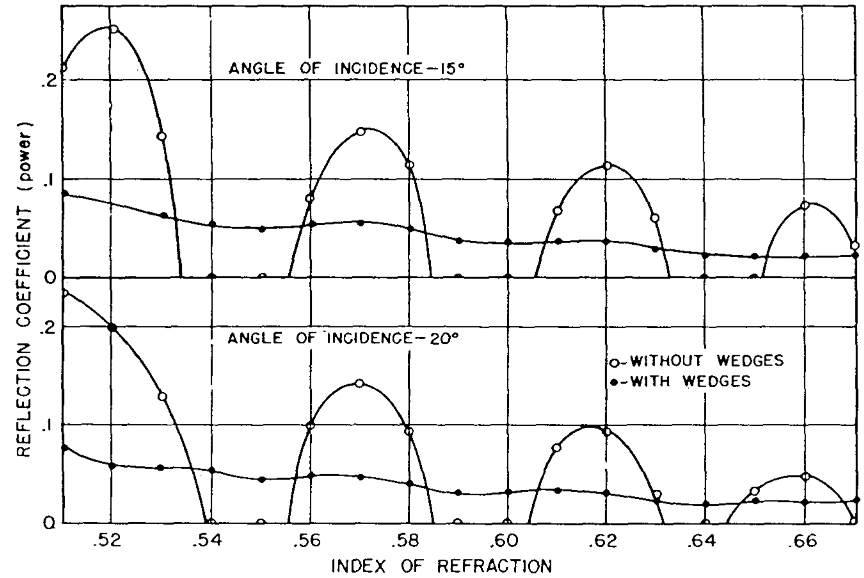

Figure 13 - Reflections from slab 6

[8] *Cf. Part 1, p. 14.*

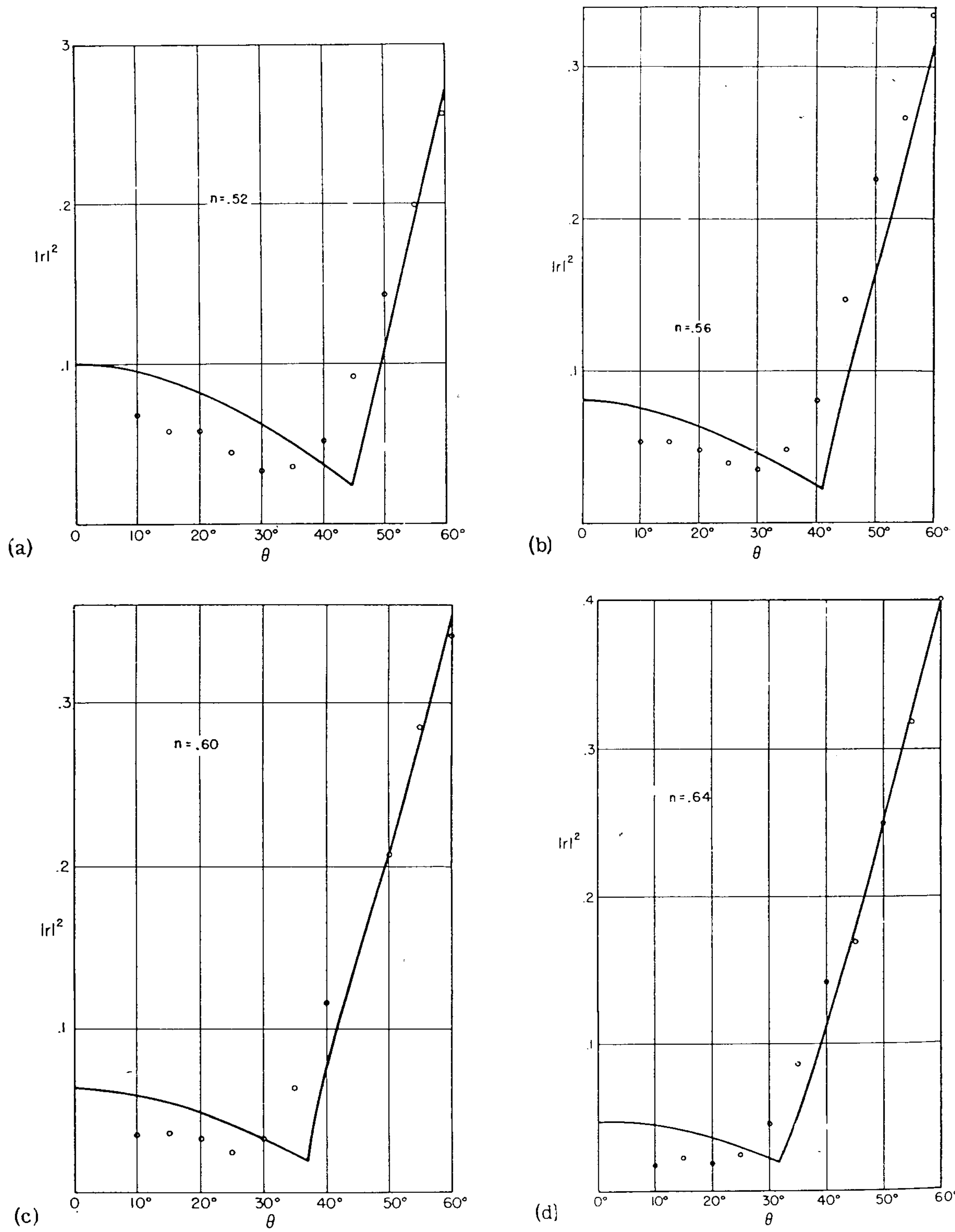

Figure 14 - Reflection as a function of the angle of incidence for n = .52, .56, .60 and .64 (Curves represent the Carlson-Heins theory)

TABLE 3
Measured Values of the (Power) Reflection Coefficient

n	θ 10	15	20	25	30	35	40	45	50	55	60
0.51	0.0766	0.0853	0.0760	0.0628	0.0480	0.0421	0.0574	0.0892	0.126	0.230	0.304
.52	.0676	.0569	.0582	.0443	.0328	.0355	.0517	.0920	.144	.199	.255
.53	.0570	.0633	.0554	.0467	.0344	.0382	.0619	.103	.183	.235	.311
.54	.0521	.0565	.0529	.0404	.0338	.0392	.0710	.125	.192	.229	.325
.55	.0445	.0489	.0449	.0368	.0322	.0402	.0683	.114	.164	.239	.282
.56	.0538	.0536	.0472	.0395	.0349	.0479	.0800	.147	.227	.266	.336
.57	.0524	.0557	.0476	.0363	.0351	.0502	.0860	.141	.175	.278	.368
.58	.0483	.0498	.0415	.0291	.0301	.0525	.0892	.140	.230	.311	.360
.59	.0384	.0384	.0302	.0244	.0300	.0592	.0970	.165	.247	.299	.348
.60	.0350	.0363	.0315	.0246	.0326	.0625	.115	.155	.206	.285	.340
.61	.0368	.0363	.0338	.0302	.0399	.0702	.113	.207	.296	.324	.368
.62	.0368	.0377	.0319	.0282	.0394	.0730	.129	.163	.200	.312	.395
.63	.0300	.0290	.0226	.0265	.0443	.0851	.133	.202	.320	.348	.379
.64	.0194	.0226	.0195	.0254	.0463	.0869	.142	.170	.250	.318	.410
.65	.0238	.0214	.0224	.0310	.0642	.0985	.150	.230	.301	.336	.360
.66	.0192	.0213	.0213	.0319	.0595	.0989	.164	.221	.283	.372	.436
.67	.0192	.0218	.0230	.0327	.0691	.131	.180	.266	.314	.378	.432

It was shown in Part 1 (p. 27) that when the angle of incidence is equal to arc cos n, the first-order diffracted beam is reflected back into the transmitter and an interesting equidistribution of power takes place, one-half of the energy being transmitted into the metal-plate medium, the other half being divided equally between the two reflected beams. As L. J. Chu pointed out, in this case the transmitted wave consists of two plane waves inclined at $\pm\theta$ to the z-axis. Within the medium the electric field is

$$i \exp (iknz) \sin \pi x/a \quad .$$

This may be written as the sum of two plane waves,

$$\tfrac{1}{2} \left\{ \exp ik (z \cos \theta + x \sin \theta) - \exp ik (z \cos \theta - x \sin \theta) \right\} \quad ,$$

which satisfy the boundary conditions on the metal plates. They will emerge at the back surface of the metal-plate medium without reflection as two plane waves of equal amplitude each carrying one fourth of the flow of energy incident on the front surface. Since back surface reflection does not occur, measurements on Slab 5 can be interpreted directly in this particular case.

The distribution of power in the presence of diffracted beams is exemplified in Figure 15. The points represent measurements on Slab 6 of the ordinary reflected and transmitted beams together with the diffracted transmitted beam. The measurement of the fourth beam had to be omitted because, for most angles of incidence shown, it was directed near the transmitter. However, the intensity of this beam was calculated, and the results are shown by a dotted line. Similar diagrams obtained for other values of the index of refraction provide a verification of Chu's prediction.

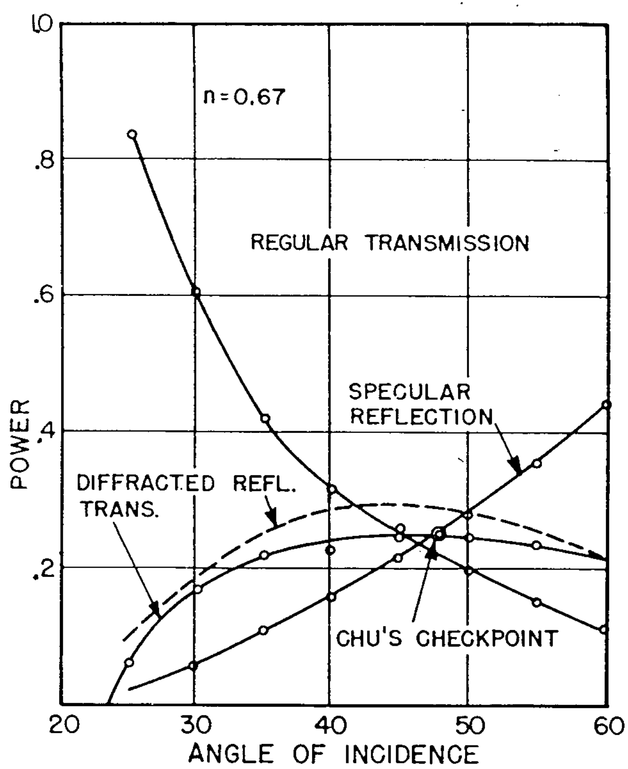

Figure 15 - Division of power for n = 0.67

SUMMARY

At normal incidence both amplitude and phase predictions of the Carlson-Heins theory have been verified experimentally for the range n = 0.35 to n = 0.67.

At oblique incidence only intensity measurements were made over the range n = 0.51 to n = 0.67. These agreed essentially with the theory, although, because of experimental difficulties, a quantitative agreement was not obtained in all cases. In particular, it has been shown that the intensity of specular reflection decreases slowly with the angle of incidence until a critical limiting angle is reached. Beyond this angle the conditions for the formation of a diffracted beam are satisfied and the intensity of the specular reflection rises sharply.

* * *

NAVY-DPPO PRNC WASH DC